RHESSI AND TRACE OBSERVATIONS OF THE 21 APRIL 2002 X1.5 FLARE

PETER T. GALLAGHER[1,2], BRIAN R. DENNIS[1], SÄM KRUCKER[3], RICHARD A. SCHWARTZ[1,4] and A. KIMBERLEY TOLBERT[1,4]

[1]*Laboratory for Astronomy and Solar Physics, NASA Goddard Space Flight Center, Greenbelt, MD 20771, U.S.A.*

[2]*L-3 Com Analytics Corp., 1801 McCormick Drive, Largo, MD 20774, U.S.A.*

[3]*Space Sciences Laboratory, University of California, Berkeley, CA 94720-7450, U.S.A.*

[4]*Science Systems and Applications, Inc., 10210 Greenbelt Road, Lanham, MD 20706, U.S.A.*

(Received 7 August 2002; accepted 23 August 2002)

Abstract. Observations of the X1.5 flare on 21 April 2002 are reviewed using the Reuven Ramaty High-Energy Solar Spectroscopic Imager (RHESSI) and the Transition Region and Coronal Explorer (TRACE). The major findings are as follows: (1) The 3–25 keV X-rays started < 4 min before the EUV (195 Å) emission suggesting that the initial energy release heated plasma directly to $\gtrsim$20 MK, well above the 1.6 MK needed to produce the Fe XII (195 Å) line. (2) Using coaligned 12–25 keV RHESSI and TRACE images, further evidence is found for the existence of hot (15–20 MK) plasma in the 195 Å passband. This hot, diffuse emission is attributed to the presence of the Fe XXIV (192 Å) line within the TRACE 195 Å passband. (3) The 12–25 keV source centroid moves away from the limb with an apparent velocity of ~ 9.9 km s^{-1}, slowing to ~ 1.7 km s^{-1} after 3 hours, its final altitude being ~ 140 Mm after ~ 12 hours. This suggests that the energy release site moves to higher altitudes in agreement with classical flare models. (4) The 50–100 keV emission correlates well with EUV flare ribbons, suggesting thick-target interactions at the footpoints of the magnetic arcade. The 50–100 keV time profile matches the time derivative of the GOES light curve (Neupert effect), which suggests that the same electrons that produced the thick-target hard X-ray emission also heat the plasma seen in soft X-rays. (5) X-ray footpoint emission has an E^{-3} spectrum down to ~ 10 keV suggesting a lower electron cutoff energy than previously thought. (6) The hard X-ray (25–200 keV) peaks have FWHM durations of ~ 1 min suggesting a more gradual energy release process than expected. (7) The TRACE images reveal a bright symmetric front propagating away from the main flare site at speeds of ≥ 120 km s^{-1}. This may be associated with the fast CME observed several minutes later by LASCO. (8) Dark sinuous lanes are observed in the TRACE images that extend almost radially from the post-flare loop system. This 'fan of spines' becomes visible well into the decay phase of the flare and shows evidence for both lateral and downward motions.

1. Introduction

On 21 April 2002, RHESSI (Lin *et al.*, 2002) observed its first X-class flare, an X1.5/1F at S14 W84. The complete rise-phase of the flare was observed by RHESSI during the daytime part of the first orbit. X-ray emission was detected from 3 keV to about 200 keV during this time. The fluxes were sufficiently high that imaging spectroscopy was possible with angular resolutions as fine as 2″ and spectral resolution of ~ 1 keV. The decay phase was clearly visible above background

CD ROM

to energies of $\gtrsim 10$ keV on subsequent orbits for the next 12 hours. This flare was also imaged by TRACE (Handy *et al.*, 1999) in its 195 Å band with $1''$ resolution and 20 s cadence, providing information on the 1.5 MK plasma from the Fe XII line emission and on the 15–20 MK plasma from the Fe XXIV emission line in the same band. A TRACE movie of this flare with RHESSI contours overlaid is available on the accompanying CD-ROM. A companion paper discusses the detailed time history of the soft and hard X-ray emission and the extent to which they show the Neupert effect (Young *et al.*, 2002).

This flare is an example of an eruptive two-ribbon long-duration event, a type C flare in the classification scheme first proposed by Tanaka (1983) and expanded by Tsuneta *et al.* (1984) and Tanaka (1987) for grouping flares according to their combined properties. It is relatively modest in peak intensity and in the maximum X-ray energies but it warrants detailed study because of the excellent coverage by RHESSI, TRACE, and other instruments. Its near-limb location allows the loops to be seen edge on and the altitude profile of the emissions to be determined into the high corona to over 140 Mm. During the rise phase, both the footpoint and the coronal X-ray emission are imaged and independent spectra can be obtained. During the long decay, the X-ray source is followed to higher and higher altitudes through the RHESSI imaging observations. The subsequent cooling of the hot loops is revealed as they appear in the TRACE passband. A fast (~ 2500 km s^{-1}) coronal mass ejection accompanied this event, which can be seen in the TRACE movie as a faint feature moving through the field of view with a velocity of ~ 120 km s^{-1}. This will be discussed further in a follow-on publication currently in preparation (Gallagher and Dennis, 2002).

Long-duration flares similar to the one reported here were studied in the 1980s with X-ray and UV instruments on the Solar Maximum Mission (e.g., Švestka *et al.*, 1982) and on Hinotori (Tsuneta *et al.*, 1984). However, they proved difficult to study with the Hard X-ray Telescope on *Yohkoh*, particularly in the decay phase, because of their large-scale structures and relatively soft spectra (Masuda, Kosugi, and Hudson, 2001). Also, the energy range of ~ 2–15 keV was not covered, thus making it difficult to image plasma in the critical temperature range of ~ 10–20 MK.

This earlier work has resulted in an understanding of such events based on the Kopp and Pneuman (1976) model of magnetic reconnection at an X-point or neutral sheet in the corona. Particles are accelerated and plasma is heated as a result of the reconnection. The accelerated electrons stream down to the footpoints and produce hard X-ray bremsstrahlung as they are thermalized by Coulomb collisions in the higher density regions of the lower corona and chromosphere. The combination of directly heated plasma already in the loop and evaporated chromospheric material (Czaykowska *et al.*, 1999) produces hot loops below the reconnection site with temperatures that can be 20 MK or higher and densities as high as 10^{13} cm^{-3}. These loops are visible in soft X-rays. They subsequently cool and eventually become visible as post-flare loops in the lower temperature EUV lines and in Hα. The reconnection site gradually moves upwards and continues to release energy, even as the total X-ray flux decreases during the decay phase of the event. This is evidenced by the appearance of higher and higher hot loops and the lower altitudes of the cooler loops. The multithermal observations reported by Švestka *et al.* (1987) show this scenario for a flare on 6 November 1980.

This paper contains the results of a preliminary analysis of the RHESSI and TRACE observations of the X1.5 flare on 21 April 2002. With the current state of our understanding of the instrument response and the capabilities of the analysis software, it is possible to obtain images at all energies where the number of counts from the flare is $\gtrsim 1000$. The highest dynamic range in any one image is currently limited to $\sim 20:1$, although image reconstruction artifacts can be present at somewhat higher levels. Currently, the shortest time resolution for obtaining an image is also limited to one spacecraft rotation period of ~ 4 s. Spectral information is available down to ~ 3 keV when all shutters are out of the field of view. However, detailed knowledge of the instrument sensitivity is still uncertain, especially at energies below 10 keV. Thus, absolute fluxes have relatively large error bars at these low energies but the images are reliable.

The following section describes the overall time-line of the flare as seen with RHESSI and TRACE. The preflare conditions and possibly related earlier flares are described. The rise phase of the flare is discussed with the appearance of hard X-ray emission and TRACE brightenings during the first RHESSI orbit. The decay phase of the flare is then discussed as it appears in hard X-rays on 7 subsequent RHESSI orbits and in the lower-temperature lines seen in the TRACE passband. In the last section, the observations are discussed in relation to possible models of energy release and particle acceleration throughout the over 12-hour duration of this event.

2. Observations

2.1. Pre-flare Activity

The period 14–21 April 2002 was a time of moderate to high solar activity, due mainly to the transit across the disk of three large regions NOAA 9901, 9906 and 9907. The X1.5 event studied here occurred in NOAA 9906 on 21 April 2002 at $\sim$00:43 UT. This region was classified as a large complex $\beta\gamma\delta$ region consisting of an asymmetric leader and follower spot with a compact area of mixed magnetic polarities in between. This can be seen clearly in Figure 1 which shows an MDI continuum image and magnetogram from the Active Region Monitor (`http://www.bbso.njit.edu/arm`; Gallagher, Moon, and Wang, 2002). Between 18 and 19 April, there was some decay evident in the interior of the group, which appears to have continued into 20–21 April, although this is difficult to confirm due to the region's proximity to the limb. When the flare started, the leader spot and

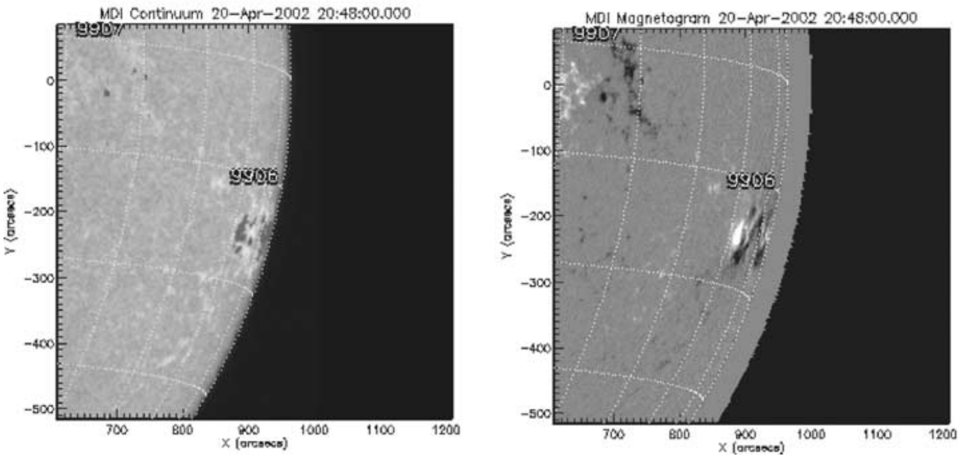

Figure 1. NOAA 9906 at 20:48:00 UT on 20 April 2002. The *left-hand panel* gives the MDI continuum image while the corresponding MDI magnetogram is given at *right*. A color version of this and other figures is on the accompanying CD-ROM.

almost 50% of the region's center had rotated off the solar disk possibly resulting in some of the X-ray emission being occulted.

The flare time-lines from GOES, TRACE, and RHESSI are shown in Figure 2. The initial activity seen in NOAA 9906 started as early as 23:00 UT on 20 April 2002 with an extremely impulsive soft X-ray event peaking at 23:27 UT. This was imaged with RHESSI as a compact source from the same location as the start of the X-flare over an hour later. This source is one of the few flares that does not show any extent beyond the finest RHESSI resolution of 2″. The small flare in the GOES time profile starting at 00:20 UT was identified as being from the opposite limb. RHESSI observed the decay phase of this event from the night-to-day transition at 00:32 UT until a second small increase was seen from NOAA 9906 starting at 00:33 UT. This decayed away until the start of the main flare.

2.2. Rise Phase

The first increase from the main flare was seen in the GOES 1–8 Å band at 00:42 UT. RHESSI saw an increase in the 3–12 keV flux starting some 2 min earlier, thus demonstrating its greater sensitivity when all shutters are out of the detector fields of view as they were at that time. The flux in this energy band rose gradually until 00:42 UT, when it became visible in the 12–25 keV band and started to rise more rapidly. The images at this time show a single source on the disc centered at heliocentric coordinates of (930″, −230″). In the top left-hand panel of Figure 3, the contours of the RHESSI image are overlaid on the TRACE image taken at the same time to within 10 s. Note that no brightening is seen in the TRACE image at this time. In fact the first increase in the 195 Å intensity was not evident until some 3 min later, at ∼ 00:45 UT. The TRACE image with the

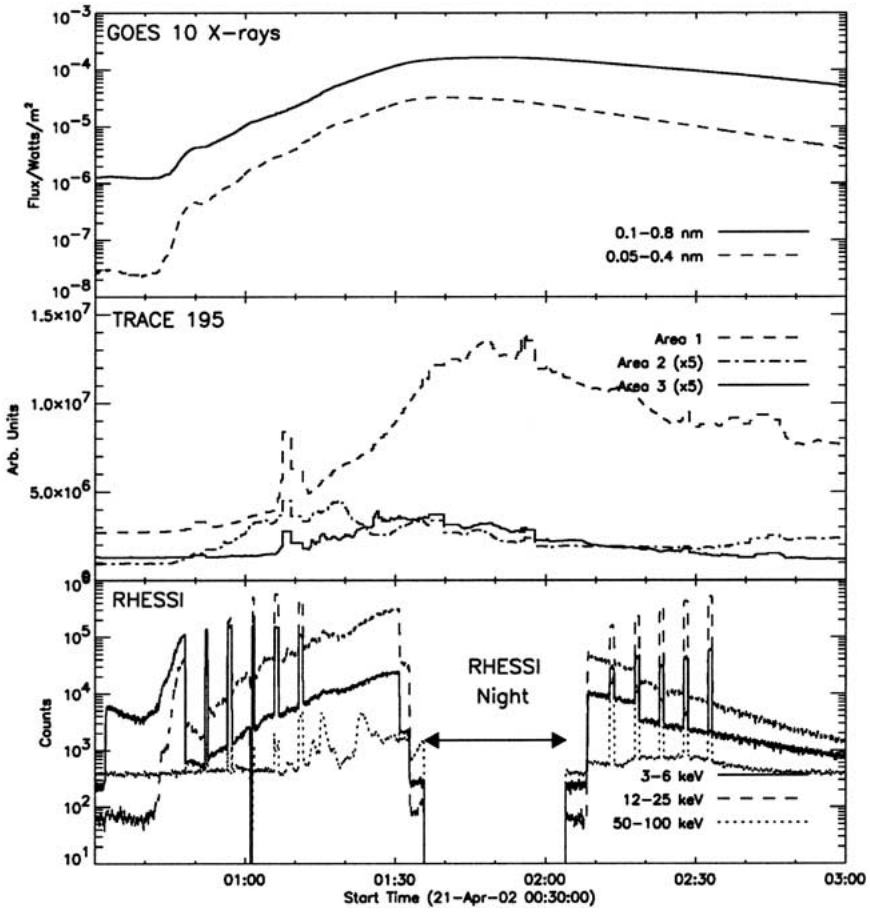

Figure 2. GOES 10, TRACE 195 Å and RHESSI lightcurves for 00:30–03:00 UT. The systematic spikes visible in the bottom panel are due to RHESSI shutter movements.

RHESSI contours overlaid at 00:48:54 UT is shown in the top right-hand panel of the same figure. As there is a small error in TRACE's pointing, the 195 Å passband images were cross-correlated with the EIT 195 Å image taken at the same time and then shifted by $\sim 2.5''$ in solar x and $\sim 4.3''$ in solar y before being coaligned with RHESSI. Further information on this technique can be found at `http://hesperia.gsfc.nasa.gov/~ptg/trace-align/`.

Once the total count rate in each of the RHESSI detector front segments reached about 20 000 counts s^{-1}, the thin shutters moved automatically into the detector fields of view. This effect can be seen clearly in the bottom panel of Figure 2. The shutters are thin discs of aluminum that absorb the lower energy X-rays and reduce the total detector count rate by a large factor. They are put in place when the counting rate becomes so high that pulse pile-up takes place causing significant spectral distortion. The effect of putting the thin shutters into the field of view can

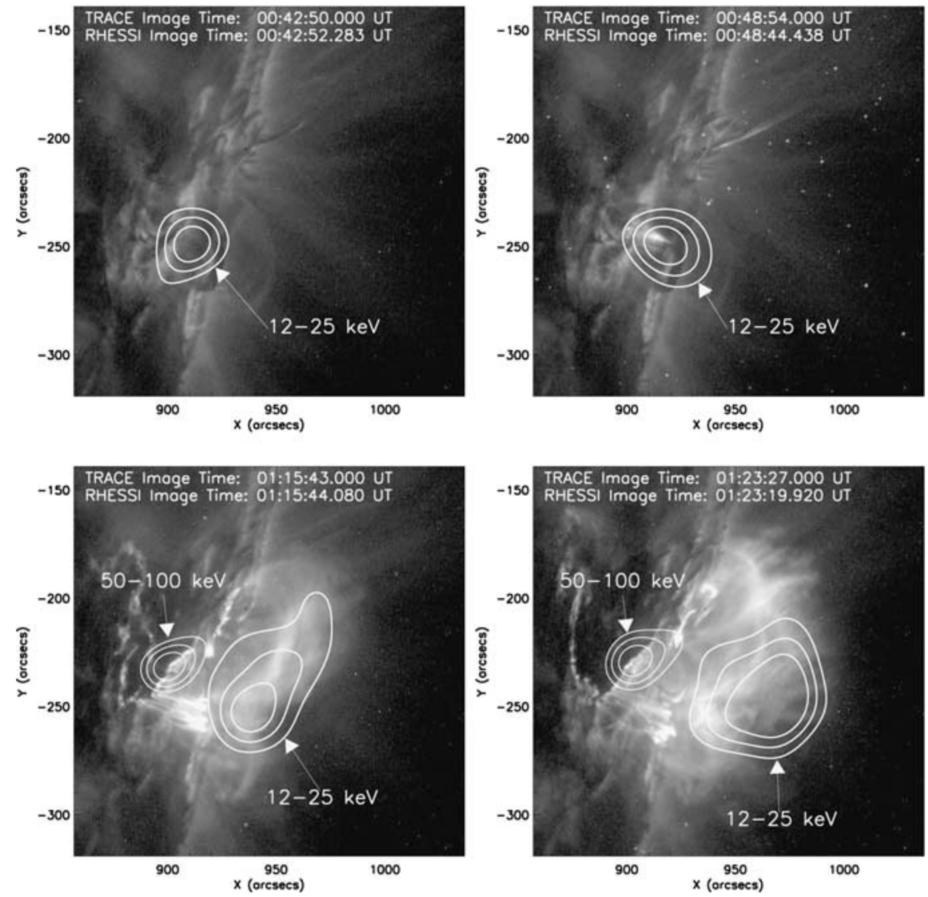

Figure 3. TRACE 195 Å and RHESSI 12–25 and 50–100 keV images for four distinctive times during the flare. The RHESSI contour levels are at 25, 50, and 75% of the peak flux for each energy band.

be seen at 00:48 UT, when the counting rate is reduced by a large factor at the lower energies. Unfortunately, the on-board algorithm that controlled the shutter movement used the now lower counting rate and determined that the shutters could be removed. Thus, after a built-in delay of 5 min the shutters were moved out. But, of course, the rate was now too high again and, after another built-in 1-min delay, the shutters were moved back in. This cycle was repeated 5 times, the maximum number allowed by the algorithm, and then finally at 01:12 UT, the shutters were put in place for the remainder of the orbit. Near the end of the daytime part of the orbit, at 01:31 UT, the total counting rate had again risen to exceed the threshold for putting the thick shutters in place, and they were automatically moved into the fields of view at that time. The same cycling of the thin shutters occurred on the next two orbits but on subsequent orbits the counting rates were sufficiently low that all shutters were removed allowing for the most sensitive observations down

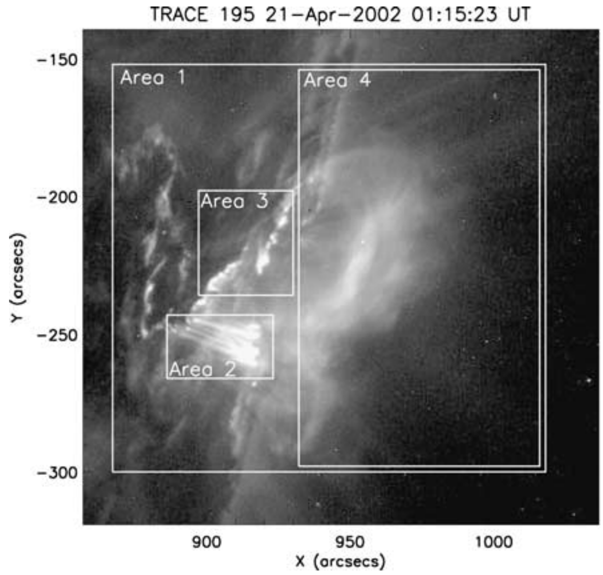

Figure 4. TRACE 195 Å image at 01:15:23 UT showing the four areas from which lightcurves were extracted. The hot, diffuse emission attributed to Fe XXIV (192 Å) is clearly visible in Area 4.

to as low as 3 keV. This sequence of shutter movements explains the large steps and peaks in the time profiles at different energies. Since the thicknesses of the shutters are accurately known from optical and X-ray measurements made before launch, the incident photon flux can still be accurately determined at all times during the event except for the times lasting for $\lesssim 1$ s when the shutters are actually moving or when pile-up becomes an issue.

The two bottom panels of Figure 3 show the RHESSI contours in the 12–25 and 50–100 keV energy bands overlaid on the TRACE images taken at the same time within 10 s. The 12–25 keV emission now extends to higher coronal altitudes and appears to show a loop-like feature connecting the initial energy release site to a point just over the limb. In the TRACE 195 Å images, this hot X-ray feature is found to be coincident with a broad area of diffuse emission which first becomes visible at $\sim$01:02 UT in the TRACE 195 Å images. This diffuse coronal brightening is believed to be from 15–20 MK plasma emitted by the Fe XXIV (192 Å) line which lies within the 195 Å band and can be seen quite clearly in Figure 4, Area 4. A similar high-temperature region was also noted by Warren and Reeves (2001) in the TRACE 195 Å passband, also near the top of a flare arcade. In this case, they derived electron temperatures of $\lesssim 20$ MK using the TRACE 195 Å/171 Å ratio for an X1.8 flare on 24 March 2000. In the bottom right-hand panel of Figure 3 at 01:23 UT, the 12–25 keV flux is now from a considerably higher altitude in the corona than seen earlier and is well above the diffuse Fe XXIV source.

The 50–100 keV emission, on the other hand, is emitted exclusively from low-altitude regions, presumably at the footpoints of the main flare arcade. When

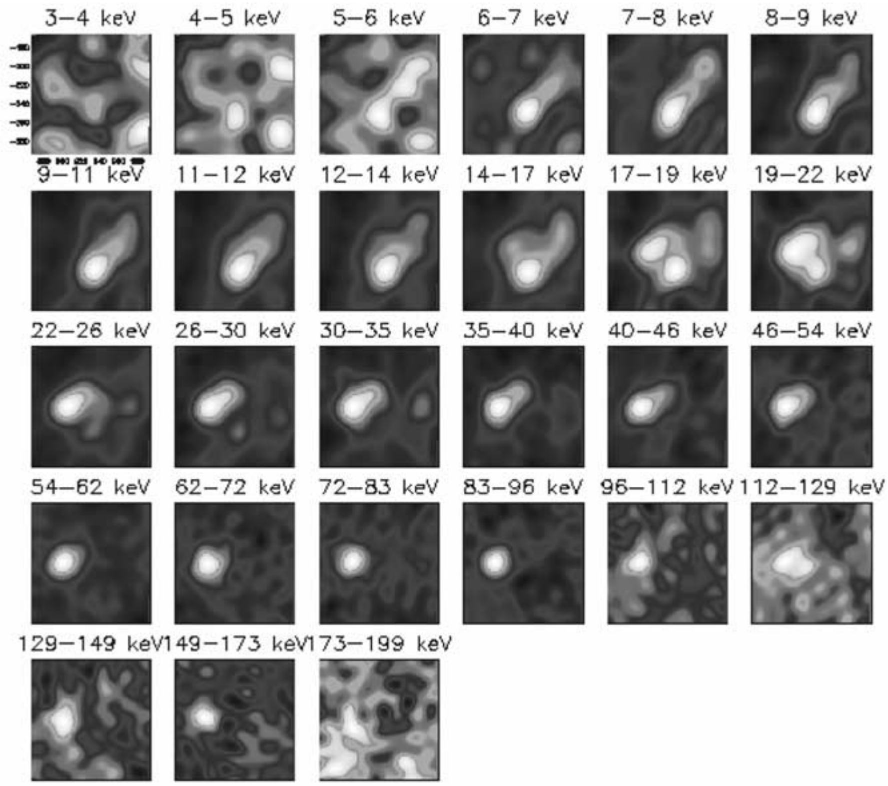

Figure 5. RHESSI images obtained in the 27 indicated energy bands using the CLEAN algorithm with collimators 3–9 for a period of 25 s (6 rotations) at the time of the peak in the hard X-ray emission near 01:15 UT. (See a color version on the CD-ROM.)

coaligned with TRACE 195 Å images, this harder emission correlates both spatially and temporally with bright EUV flare ribbons. This is consistent with models in which flare-accelerated electrons stream down magnetic field lines and lose their energy in the higher densities of the chromosphere. This then results in heating of the chromospheric plasma to coronal temperatures and the formation of bright flare ribbons, visible in numerous lines, including Hα (Qiu *et al.*, 2001). In the images on the bottom panels of Figure 3, the hard X-ray emission can be seen overlying the EUV flare ribbons, which are presumably heated by the same flare electrons.

Various peaks in the hard X-ray emission were seen up to the 100–300 keV energy band, most notably at 01:15 UT and again at 01:23 UT. The time profile for the complete rising phase of the flare was characterized, however, by gradual variations; the most impulsive emission, even at the highest energies, had timescales not much shorter than 1 min. We have looked in detail at the first of these peaks. The RHESSI images in Figure 5 for this peak show that the X-ray source can be located with $\lesssim 5''$ accuracy in all energy bands from 6–173 keV. At the higher energies above ~ 50 keV, the source is unresolved at the $7''$ resolution of these

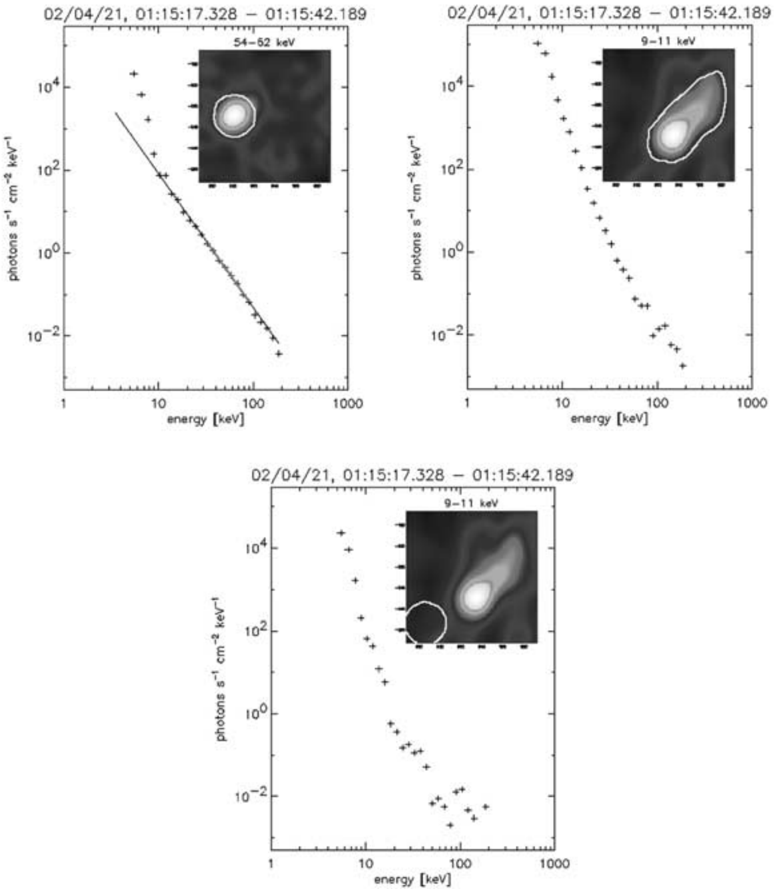

Figure 6. Spectra of the two bright sources seen in the images of Figure 5. *Top left*: the source on the solar disk with an $E^{-3.2}$ power-law fit between 30 and 100 keV. *Top right*: the coronal source with an E^{-7} power-law fit from 8–30 keV. *Bottom*: the spectrum from the indicated region well away from either of the two bright sources. (A color version on the CD-ROM.)

images. It is located on the solar disk coincident with the EUV ribbons seen in the TRACE images, presumably at the foot points of the arcade of magnetic loops. At lower energies, below about 14 keV, the source is at a different location above the limb. Both sources are evident in the transition that takes place in the images between ~ 14 and ~ 46 keV.

The spectra of these two different sources in this same time interval are shown in Figure 6. The spectrum of the source on the disk is shown in the top left of Figure 6. Between 30 and 100 keV, a power-law function with an index of -3.2 provides a good fit to the data points. The spectrum of the coronal source is shown to the right. It can be fitted with an E^{-7} power law between 8 and 30 keV. Note that the spectrum of the disk source steepens to about this same E^{-7} form below about 15 keV whereas the spectrum of the coronal source flattens to about an E^{-3}

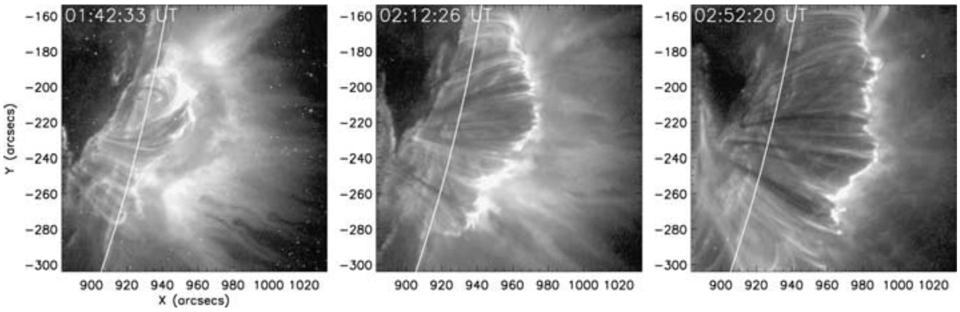

Figure 7. Rising post-flare loop system seen in TRACE 195 Å from 01:42 UT to 02:52 UT.

form above about 50 keV. This effect seems to be caused by contamination of the spectrum of one bright source by a background from the other bright source. That such a background is present in the images can be seen from the spectrum shown in the lower panel of Figure 6. This is from the indicated region that appears free from either of the two bright sources and yet it has a similar steep spectrum at lower energies that becomes flatter at higher energies.

We conclude from these spectra that it is not possible to determine, at this stage in the evolution of the data analysis procedures, if the coronal source is a thermal exponential or a nonthermal power law. It is not yet clear exactly what background must be subtracted from the spectrum determined from the location of the coronal source at the higher energies. Detailed modeling is probably the only way that this question can be answered.

It seems clear, however, that the footpoint source spectrum extends down to as low as 10 keV with the same $E^{-3.2}$ spectrum as seen to energies at least as high as 100 keV. If this is correct, then it would indicate that the spectrum of the precipitating electrons must extend down to at least this energy without a turnover. This is a factor of at least two lower in energy than that often assumed for the cutoff in the electron spectrum, thus leading to a factor of 5 greater energy in electrons than would have been calculated with the higher cutoff energy.

The softer X-ray emission continued to rise monotonically for the remainder of the daytime part of the RHESSI orbit that ended at 00:01:37 UT. The GOES light curves show that the peak was reached at 01:50 UT. Thus, the rise phase of the flare lasted for 70 min. The temperature at this time derived from the ratio of the fluxes in the two GOES channels was 17 MK and the emission measure was 2×10^{50} cm^{-3}.

2.3. Decay Phase

The decay phase of the flare lasted for a further 14 h or at least until 16:00 UT. There is a notable lack of smaller events during this period compared with the earlier and later average rates of such events. Only two or three small events are

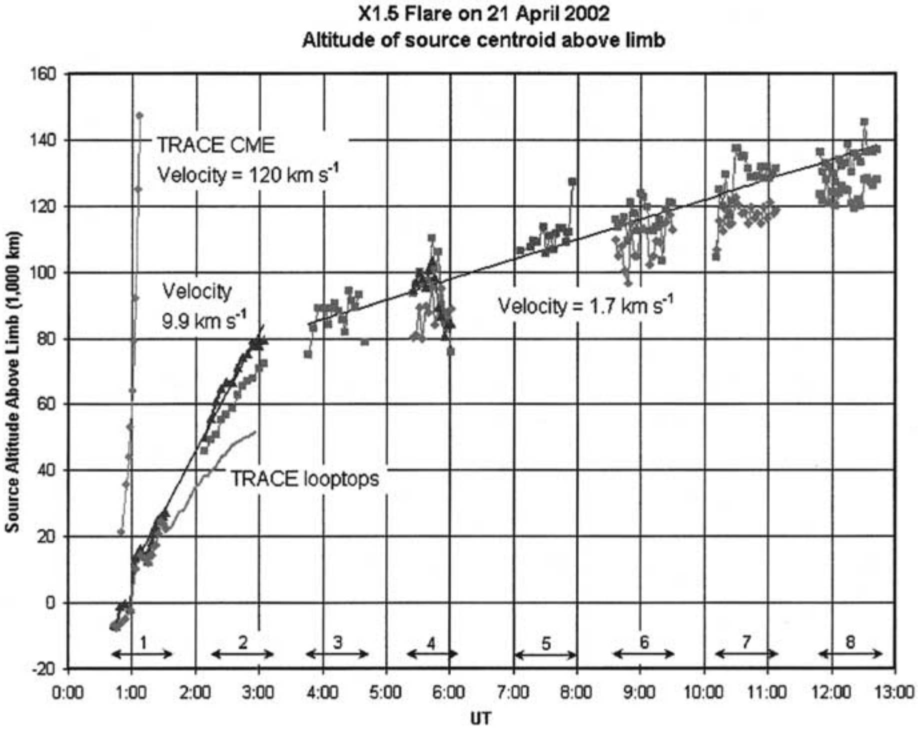

Figure 8. Apparent altitude above the solar limb as a function of time for several features seen in RHESSI and TRACE images. The RHESSI 3–6, 6–12, and 12–25 keV source centroids are indicated by *diamonds*, *squares*, and *triangles*, respectively.

seen in the GOES plot above the decaying flux from the main event, suggesting that additional activity was suppressed during this 16-hour interval.

RHESSI observations are available up until almost 13:00 UT after which the data are missing. The thin shutters were in the detector fields of view for the first two orbits of the decay (apart from five 1-min intervals when they were moved out as discussed above). On the five subsequent orbits, all the shutters were out of the field of view and the flare emission is seen above background below 10 keV for the whole time.

Of particular interest during the decay phase is the rise of the sources of emission, both in X-rays as seen with RHESSI and in the EUV as seen with TRACE. Figure 7 shows the rising post-flare loop system as seen by TRACE at approximately 1, 1.5, and 2 h after the flare begins. We have made images with RHESSI throughout the decay phase in the 3–6, 6–12, and 12–25 keV energy bands. For each image, we have determined the location of the centroid of the emission inside the contour level at 50% of the peak value in each image. Since the source is about 20″ in extent during this whole period with no evidence of any finer structure, we have used only the detectors behind collimators 6–9 to make the images. We used the back-projection image reconstruction technique for speed since we were not concerned with the side lobes that were always below the 50% level.

Figure 8 shows the computed height of the centroid above the limb in the plane of the sky. A similar analysis has been done for the TRACE images for both the post-flare loops and a faint CME-like feature observed propagating away from the main flare site. The resultant altitudes above the limb are plotted on the same figure for comparison with the X-ray information. Detailed analysis of the X-ray centroid locations and their movements with time shows immediately that they all rise to higher and higher altitudes above the limb, reaching over 140 000 km. The X-ray centroids rise initially at a rate of about 10 km s^{-1} until about 03:00 UT and then slow down to about 1.7 km s^{-1} for the rest of the time. Note that the lower-energy X-ray centroids are consistently at a lower altitude than the higher-energy centroids. The centroids of the 12–25 keV X-rays are about 10 000 km lower than the 6–12 keV centroids during the second orbit from 02:00 to 03:00 UT. The 3–6 keV centroids are about 10 000 km below the 6–12 keV centroids after 05:15 UT. Similar motions of the TRACE features are also seen in the figure. The post-flare loop tops rise rapidly between approximately 01:00 and 03:00 UT although at a slightly slower rate than the X-ray features seen in RHESSI. The Fe XII loop-tops are always well below the centroids of the X-ray emission. This pattern of higher loops being hotter than the loops below them is consistent with the flare scenario described above.

Also plotted in Figure 8 are heights as a function of time of a faint feature ejected from the main flare site at the flare onset time. Due to the morphology, timing and direction of this fast-moving feature, it is almost certainly associated with a fast CME observed to have velocities of $\sim$2500 km s^{-1}. In TRACE the measured velocity was $\sim$120 km s^{-1} (Gallagher and Dennis, 2002).

At any given time, the energy release site is at or above the highest sources that are observed. This site is rising continuously and the released energy results in higher and higher loops becoming filled with hot plasma. The newly heated loops appear first in X-rays. The lower energy X-ray source and the TRACE features are loops that have cooled to temperatures at which these band passes are sensitive. An estimate can be made of the loop cooling times from the altitudes and times at which they are seen in the different temperature regimes.

3. Summary and Conclusions

It is clear that RHESSI's imaging and spectroscopic capabilities are already providing new insights into high-energy processes in solar flares, such as particle acceleration, propagation, and precipitation. In combination with observations from ground- and space-based observatories such as SOHO and TRACE, it is now possible to gain an unprecedented understanding of flaring plasmas from the corona, through the transition region, to the chromosphere. In this paper, soft and hard X-ray images and spectra from RHESSI together with EUV images from TRACE were used to study the X1.5 of 21 April 2002. The major findings are as follows:

(1) The 3–25 keV X-rays started <4 min before the EUV (195 Å) emission at the same location. This suggests that the initial energy release heated plasma directly to ~ 20 MK, well above the 1.5 MK needed to produce the Fe XII emission line at 195 Å. Presumably it took several minutes for a sufficient amount of plasma to cool down to be visible in Fe XII. The Fe XXIV resonance line at 192 Å from 15 MK plasma must have been too weak to be detectable with TRACE in the 195 Å band although it is not clear what line produced the first detectable EUV emission.

(2) Some parts of the flare may have been occulted by the solar limb. There is some evidence for this in EUV brightenings at and above the limb earlier than, and at a different location to that of the initial X-ray brightening. Also, the appearance of the high-altitude Fe XXIV and 12–25 keV X-ray emissions later in the flare suggests a large loop-like structure extending beyond the limb. It is not clear what effects the over-the-limb parts of the flare could have had on the appearance of the flare as seen with RHESSI and TRACE, although the indications are that they were probably not major. Based on the earlier longitudinal extent ($\sim 200''$) of this active region (NOAA 9906) when it was all visible on the disk 1 day earlier, it is unlikely that any part of the flare was more than about $50''$ over the limb.

(3) The 3–25 keV X-rays came from higher and higher altitudes as the flare progressed. The 12–25 keV source centroid moved away from the limb at an apparent velocity of 9.9 km s^{-1} from 01:00 to 03:00 UT. The velocity decreased at about this time to 1.7 km s^{-1} and continued at this rate until at least 13:00 UT, when the source of 6–12 keV X-rays was at $\sim 140\,000$ km above the limb. This suggests that the energy release site moved to higher altitudes also.

(4) During the rise and early decay phase of the flare, the 12–25 keV source was at the same or greater altitude above the limb as the source of the Fe XXIV emission, and both were well above the tops of the Fe XII loops. By 03:00 UT, the 12–25 keV source was at 80 000 km above the limb while the Fe XII source was at 50 000 km. Later in the decay phase, the 3–6 keV source was consistently about 10 000 km lower than the 6–12 keV source. All of these observations are consistent with the generally held picture of a rising energy release site that heats the magnetic structures below it. These then cool and become visible at the lower temperatures. It is not clear if there is any relation between the velocity of the energy release site and the velocity of the associated CME or why the velocity changed quite abruptly at about 03:00 UT from 10 to 1.7 km s^{-1}. Also, why should the energy release on the decay be so smooth compared to the relatively impulsive release on the rise?

(5) The ≥ 25 keV X-ray emission later in the flare came from the location of the ribbons seen in the TRACE images suggesting electron beams and thick-target interactions at the footpoints of the magnetic arcade of loops. The 50–100 keV time profile matches the time derivative of the GOES light curve (Neupert effect; see Young *et al.*, 2002). This suggests that the same electrons that produced the thick-target hard X-ray emission also heat the plasma that is seen in the GOES soft X-ray

emission. The peak temperature derived from the GOES 2-channel measurements is 17 MK and a peak emission measure of 2×10^{50} cm^{-3}.

(6) X-ray footpoint emission has an $E^{-3.2}$ spectrum all the way down to ~ 10 keV suggesting a lower electron cutoff energy than previously thought. This results in a factor of $(20/10)^{2.2} \approx 5$ greater energy in the electrons than if a 20 keV cutoff were assumed as has generally been used in the past. However, this increase in total energy in electrons is offset by the steep spectrum (E^{-7}) of the emission from high in the corona that would dominate the spatially integrated spectrum below 25 keV. It should be possible to estimate the total time-integrated energy in the electrons that produced this emission assuming a 10 keV cutoff energy.

(7) There was no impulsive X-ray emission with time constants of much less than 1 min. The main hard X-ray (25–200 keV) peaks have FWHM durations of ~ 1 min. This suggests a more gradual energy release process, possibly reflecting weaker than usual magnetic fields and the increasing altitude of the energy release site.

(8) The TRACE images reveal a 'feature' propagating outward into the corona at a speed of $\gtrsim 120$ km s^{-1} following the initial brightening. The time and place of origin of this feature is not clear, nor is its physical interpretation. This may be connected to the coronal mass ejection seen with LASCO following the flare with a very high velocity of 2500 km s^{-1}. Extrapolating the LASCO height-time profile to the solar surface reveals a start time of 01:13 UT, some 30 min after the start of the X-ray event. From the TRACE height-time profile, it is clear that height $\sim$ time$^{\alpha}$, where $\alpha > 1$. This therefore places the CME launch time closer to the flare peak (Gallagher and Dennis, 2002).

(9) Dark sinuous lanes that seem to be propagating downwards from the high corona appear in the TRACE images after the peak of the soft X-ray event. These features are similar to those observed previously in *Yohkoh*/SXT images, which McKenzie and Hudson (1999) attributed to downward propagating voids created by evacuated flux tubes. Švestka *et al.* (1998), on the other hand, speculate that this 'fan of spines' represents a set of mini-streamers or extensions similar to polar plumes. Our preliminary analysis indicate that theses features are most likely due to the presence of downward propagating voids or cool material. An interesting possibility is that these alternating dark and bright spines are generated by an MHD Kelvin–Helmholtz type shear instability similar to that described by Andries, Tirry, and Goossens (2000) and Andries and Goossens (2001) for plumes.

4. Future Work

This paper has provided an overview of the new RHESSI and TRACE observations of the X1.5 flare on 21 April 2002. Many conclusions are obvious from the preliminary analysis of these two data sets that we have been able to do so far. Thus, we feel it is useful to publish these early results. Clearly, further work can be done once more refined analysis procedures are perfected and the RHESSI instrument responses are more accurately and reliably understood. In particular, further analysis of the rise phase offers new insights into the electron acceleration and heating processes going on at this time. The association between these traditional flare phenomena and the apparently near simultaneity of the CME onset as seen in the TRACE movie is particularly intriguing.

Many advanced analysis tools are now becoming available for RHESSI. Recently, it has been possible to include collimators 1 and 2 in the image reconstruction process, thus allowing the possibility of obtaining images for this flare with up to $2''$ resolution, at least a factor of 3 better than the images presented here. Also, knowledge of the instrument response function is being improved, particularly at energies below 10 keV, where most of the emission was recorded in the decay phase of this event. Modeling of sources similar to those observed here is ongoing to determine what features are real and what are artifacts of the image reconstruction algorithm. This should also allow for a better understanding of the backgrounds underlying the sources in the images and how best to obtain the spectrum of each source region free from contamination from other sources in the image. As knowledge of the grid modulation parameters improves, it should be possible to increase the image dynamic range towards the design goal of 100:1, thus making source contamination less of a problem. Other image reconstruction algorithms can also be tried such as maximum entropy, forward fitting (Aschwanden *et al.*, 2002), and pixons. These may well be better suited to providing more accurate photometry than the CLEAN algorithm used for the images shown in this paper. For TRACE, we will determine the sensitivity of the 195 Å bandpass and compare the emission measure from its flux to the temperature and emission measure of the near cospatial source seen with RHESSI.

Acknowledgements

The authors would like to thank the referee, František Fárník, and RHESSI team-member, Hugh Hudson, for their comments and discussion during the preparation of this work.

References

Andries, J. and Goossens, M.: 2001, *Astron. Astrophys.* **368**, 1083.
Andries, J., Tirry, W. J., and Goossens, M.: 2000, *Astrophys. J.* **531**, 561.
Aschwanden, M. J., Schmahl, E., and the RHESSI Team: 2002, *Solar Phys.*, this volume.
Czaykowska, A., De Pontieu, B., Alexander, D., and Rank, G.: 1999, *Astrophys. J.* **521**, L75.
Gallagher, P. T. and Dennis, B. R.: 2002, *Astrophys. J.*, in preparation.
Gallagher, P. T., Moon, Y.-J., and Wang, H.: 2002, *Solar Phys.* **209**, 169.
Handy, B. N. *et al.*: 1999, *Solar Phys.* **187**, 229.

Kopp, R. A. and Pneuman, G. W.: 1976, *Solar Phys.* **50**, 85.
Lin, R. P. *et al.*: 2002, *Solar Phys.*, this volume.
Masuda, S., Kosugi, T., and Hudson, H. S.: 2001, *Solar Phys.* **204**, 57.
McKenzie, D. E. and Hudson, H. S.: 1999, *Astrophys. J.* **519**, L93.
Qiu, J., Ding, M. D., Wang, H., Gallagher, P. T., Sato, J., Denker, C., Goode, P. R.: 2001, *Astrophys. J.* **554**, 445.
Švestka, Z., Stewart, R. T., Hoyng, P., van Tend, W., Acton, L. W., Gabriel, A. H., Rapley, C. G., Boelee, A., Bruner, E. C., de Jager, C., Lafleur, H., Nelson, G., Simnett, G. M., van Beek, H. F., and Wagner, W. J.: 1982, *Solar Phys.* **75**, 305.
Švestka, Z. F., Fontenla, J. M., Machado, M. E., Martin, S. F., Neidig, D. F., and Poletto, G.: 1987, *Solar Phys.* **108**, 237.
Švestka, Z. F., Fárník, F., Hudson, H. S., and Hick, P.: 1998, *Solar Phys.* **182**, 179.
Tanaka, K.: 1983, in P. B. Byrne and M. Rodono (eds.), 'Activity in Red-Dwarf Stars', *IAU Colloq.* **71**, 307.
Tanaka, K.: 1987, *Publ. Astron. Soc. Japan* **39**, 1.
Tsuneta, S.: 1997, *Astrophys. J.* **483**, 507.
Tsuneta, S., Takakura, T., Nitta, N., Ohki, K., Tanaka, K., Makishima, K., Murakami, T., Oda, M., and Ogawara, Y.: 1984, *Astrophys. J.* **280**, 887.
Warren, H. P. and Reeves, K. K.: 2001, *Astrophys. J.* **554**, L103.
Young, C. A., Dennis, B. R., Schwartz, R. A., and Tolbert, A. K.: 2002, *Solar Phys.*, in preparation.